Experimental investigation of a virtual planar array for MIMO sonar systems

Sven Schröder, Jens Reermann, Sarah Barnes, et al.

Citation: Proc. Mtgs. Acoust. **47**, 070005 (2022); doi: 10.1121/2.0001591
View online: https://doi.org/10.1121/2.0001591
View Table of Contents: https://asa.scitation.org/toc/pma/47/1
Published by the Acoustical Society of America

Volume 47 http://acousticalsociety.org/

International Congress of Underwater Acoustics
Southampton, UK
20-23 June 2022

Underwater Acoustics: Transducer and array technology

Experimental investigation of a virtual planar array for MIMO sonar systems

Sven Schröder
Department of Methods and Processing, German Aerospace Center DLR Institute for the Protection of Maritime Infrastructures, Bremerhaven, Bremen, 27572, GERMANY; sven.schroeder@dlr.de

Jens Reermann
ATLAS ELEKTRONIK GmbH, Bremen, GERMANY; jens.reermann@atlas-elektronik.com

Sarah Barnes
German Aerospace Center DLR Institute for the Protection of Maritime Infrastructures, Bremerhaven, Bremen, GERMANY; sarah.barnes@dlr.de

Dieter Kraus
City University of Applied Sciences: Hochschule Bremen, Bremen, GERMANY; dieter.kraus@hs-bremen.de

Anton Kummert
Bergische Universität Wuppertal Fachbereich E Elektrotechnik Informationstechnik Medientechnik: Bergische, Wuppertal, North Rhine-Westphalia, GERMANY; kummert@uni-wuppertal.de

In this paper a way to achieve a virtual two-dimensional planar array for sonar systems using the multiple input multiple output (MIMO) principle is presented. The time delay information of a planar array can be used for imaging sonars and allows the localization of scatterers in three-dimensional space. In a conventional single input multiple output (SIMO) sonar, this would be achieved using a single transmitter and a receiver consisting of a planar array of N^2 hydrophones, arranged as a rectangular $N \times N$ matrix. We show through simulations and experiments how a virtual planar array can be formed using a linear receiver array and linear transmitter array. For this, an experimental MIMO sonar system was constructed with a 32-channel receiver and a 12-channel transmitter, which allowed the realization of a virtual 32×12 array. The array design is analyzed through experiment in a harbor basin and through simulations, validating the principle of the virtual planar array. In addition to the experimental investigations, in which only a limited number of transmitter channels are available, further simulations with a 32×32 array are performed for further MIMO arrangements to highlight strengths and weaknesses in different application areas.

Published by the Acoustical Society of America

 https://doi.org/10.1121/2.0001591

1. INTRODUCTION

An active sonar emits acoustic waves to detect and locate underwater objects and structures. A conventional active sonar usually consists of a transmitter unit and a receiver array. The transmitter unit can be considered as a point source with a certain directional characteristic, which emits acoustic energy into an area using a transmitter pulse, e.g. a Continuous Wave (CW) or Frequency Modulated (FM) pulse [1]. It can be considered as a single input to the acoustic channel. In the acoustic channel the signal passes through a medium (water), is backscattered from objects, the seafloor, water surface and by the medium itself, and is received by the elements of the receiver array. The receiver elements can be interpreted as multiple outputs of the acoustic channel. Therefore the conventional active sonar system is called Single-Input-Multiple-Output (SIMO) sonar. Using the travel time information of the transmitted pulse, the localization of objects can be estimated by beamforming techniques, where the range resolution depends on the bandwidth of the transmitted pulse, while the angular resolution depends on the aperture length of the receiver array and the number of receiver elements.

To reconstruct the backscattered sound in a three-dimensional space, e.g. for acoustic cameras, the information of range, azimuth and elevation has to be obtained for which a two-dimensional array is needed. A simple arrangement is a planar, rectangular grid with N_r rows and N_c columns, which are filled with $N = N_r N_c$ receivers and one transmitter. This SIMO arrangement has the disadvantage that electroacoustic transducers, analog signal conditioning and analog-to-digital converters (ADC) are required for each of the large number of receiver channels, resulting in a complex and expensive design. A simpler, less expensive alternative can be found by using of the novel multiple-input multiple-output (MIMO) sonar approach [2,4–6], which can create a virtual planar array using a linear receiver and transmitter array. Here, a large number of transmitters emit different, ideally orthogonal, transmitter pulses, which can be separated from each other in the receiver-side signal processing. Therefore, signal separation plays a key role in this process.

In this paper, an overview of the concept of a virtual planar array is given in Section 2. Following this, in Section 3 a set of Orthogonal-Frequency-Division-Multiplexing (OFDM) signals are presented, for use with the multiple transmitters in a MIMO sonar setup. In Section 4 the principle of a virtual planar array is tested through simulations and compared to conventional SIMO arrays. Furthermore, a MIMO sonar demonstrator was built which allowed us to perform experiments in a realistic environment in a harbor basin and to validate results of the previously performed simulations, which is shown in Section 5. Finally, the work is summarized in Section 6.

2. CONCEPT OF A VIRTUAL PLANAR ARRAY

The monostatic sonar system considered within this work has M transmitters and N receivers, which are located at the positions $\mathbf{q}_{T,m} \in \mathbb{R}^3$ with $m = 0, ..., M-1$, and $\mathbf{q}_{R,n} \in \mathbb{R}^3$ with $n = 0, ..., N-1$. In a general static scenario the relationship between the mth transmitter and the nth receiver can be described by the impulse response $h_{mn}(t)$. The nth receiver signal resulting from the superposition of all transmitter signals $s_m(t)$ after passing through the acoustic channel can be expressed by

$$s_n(t) = \sum_{m=0}^{M-1} (s_m * h_{mn})(t), \tag{1}$$

where (*) is the convolution operator. In an ideal channel with K point scatterers at the locations $\mathbf{q}_{S,k} \in \mathbb{R}^3$ with $k = 0, ..., K-1$, (1) can be described in detail by

$$s_n(t) = \sum_{m=0}^{M-1} \sum_{k=0}^{K-1} a_{mnk} \cdot s_m(t - \tau_{mnk}), \tag{2}$$

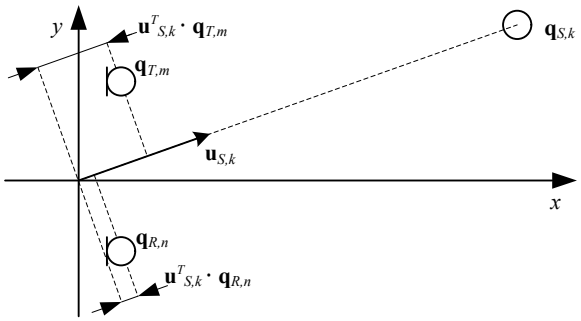

Figure 1: Approximation of the travel path in a far field scenario

with the propagation losses a_{mnk} and the travel time

$$\tau_{mnk} = \frac{|\mathbf{q}_{T,m} - \mathbf{q}_{S,k}| + |\mathbf{q}_{R,n} - \mathbf{q}_{S,k}|}{c} \tag{3}$$

between transmitter, scatterer and receiver, where c is the speed of sound. For a scatterer located in the far-field, (3) can be approximated by

$$\tilde{\tau}_{mnk} = \frac{2\,|\mathbf{q}_{S,k}| - \mathbf{u}^T_{S,k}\,(\mathbf{q}_{T,m} + \mathbf{q}_{R,n})}{c}, \tag{4}$$

where $\mathbf{u}_{S,k} = \mathbf{q}_{S,k}/\,|\mathbf{q}_{S,k}|$ is a unit vector, which points in the direction of the scatterer (cf. Fig. 1). Here it becomes clear, that the same travel time information can be obtained by a virtual array with NM elements at the positions

$$\mathbf{q}_{V,mn} = \{\mathbf{q}_{T,m} + \mathbf{q}_{R,n} | m = 0, ..., M-1; n = 0, ..., N-1\}. \tag{5}$$

Thus, by careful arrangement a virtual planar array with MN elements can be created by only using $M + N$ physical transducers.

3. TRANSMITTER SIGNALS

A key element of MIMO systems is the design of transmitter signals, since the separability of the transmitter signals in the receiver signal processing is essential for the functionality of the system. In the literature, methods for signal separation are often divided into Time-Division-Multiple-Access (TDMA), Frequency-Division-Multiple-Access (FDMA) and Code-Division-Multiple-Access (CDMA) approaches [7].

Using the TDMA method, all transmitter signals use the same frequency band, but different time slots. The time slots are carefully arranged to ensure that the signals are distinguishable at the receiver, therefore a previous knowledge of the acoustic channel is necessary. The sequential transmission of the signals leads then to a perfect signal separation, but since time passes between the single measurements the channel can change, e.g. due to the movement of the target. In addition, the duration of the transmission sequence and thus the ping period increases with the number of transmitters.

In the FDMA method, signal separation is achieved by dividing the transmitter frequency band into sub frequency bands, in which the transmit signals are distributed. This allows simultaneous transmission and in theory a perfect signal separation. However, the bandwidth of electroacoustic transducers is usually very limited, thus dividing the available frequency band by the number of transmitters further limits the bandwidth of the transmitted pulses, which reduces the range resolution accordingly.

With the CDMA method all transmitters use the same time slot and frequency band, whereby signal separation is accomplished using coding techniques. The advantage of the CDMA method is that it allows a large number of transmitters without having to restrict the transmission duration or bandwidth of the respective transmission pulses, as would be the case with TDMA and FDMA. However, this also has the consequence that many transmitters radiate their energy at the same time in the same frequency spectrum and the separation of the signals is only possible to a limited extent. The signal separation is realized by using matched filter banks in the receiver signal processing, which provide a correlation between the received signal and the transmitted signals. Therefore, the properties of the cross correlations between the transmitter signals determine the property of the signal separation [8].

In this demonstration the CDMA method is used to separate transmitter signals. For this purpose a set of orthogonal-frequency-division (OFDM) signals is designed. OFDM signals originated in communications technology and represent a comparatively new field of research for application in radar systems [9]. The principle is based on a multiplexing method using orthogonal carrier frequencies. For this purpose, the transmitter frequency band is divided into sub frequency bands B_{sub}, whose bandwidth depends on the length of the OFDM signal via the orthogonality condition

$$T = \frac{1}{B_{\mathrm{sub}}}, \tag{6}$$

where T is the length of the OFDM pulse (symbol). If this condition is fulfilled, then in the frequency domain the carrier frequencies are located in the first zero crossings of the sinc function of the adjacent carrier frequencies. In the time domain, each carrier frequency has an integer number of periods. In the present work, 32 OFDM pulses are used as transmitter pulses, which are generated by

$$s(t) = \sum_{n=0}^{N_c-1} c_n \cdot e^{j2\pi f_n t} \tag{7}$$

with

$$f_n = f_0 + n \cdot B_{\mathrm{sub}} \quad \text{and} \quad N_c = B \cdot T, \tag{8}$$

where $B = N_c B_{\mathrm{sub}}$ is the bandwidth, f_0 the first center frequency of the fist sub band, and the sequence $c_n \in \{-1, 1, -j, j\}$ for $n = 0, ..., N_c - 1$, resulting in each carrier frequency containing two bits of information.

4. SIMULATION

To verify the concept of the virtual planar array, a simulation was built in python based on the MIMO channel described in (2). Thereby, the signals of the paths between each transmitter and receiver are calculated. The simulated receiver signal is then obtained by superimposing the individual signal paths. In this simulation, three different scenarios of a 32×32 array are considered. In the first scenario, a conventional 32×32 receiver array is considered (cf. Figure 2.a), which represents a single-input multiple-output (SIMO) case and can be used as a reference for further analysis. In the second scenario, the simplest form of a MIMO array with a virtual aperture of 32×32 channels is realized by a T array. It consists of 32 receivers arranged horizontally and 32 transmitters positioned vertically above the receiver array (cf. Figure 2.b). This setup has the smallest ratio between the number of physical transducers required and the number of virtual array elements achieved. However, this setup requires 32 transmitter signals to be emitted simultaneously and generating significant uncorrelated noise due to crosstalk between the transmitter signals (cross-correlation noise). Therefore, in the last scenario, an H arrangement as shown in Figure 2.c is used. This arrangement halves the number of transmitters needed, which also reduces the influence of cross-correlation noise. However, 16 additional transducers are required for this setup, increasing the ratio of electroacoustic transducers

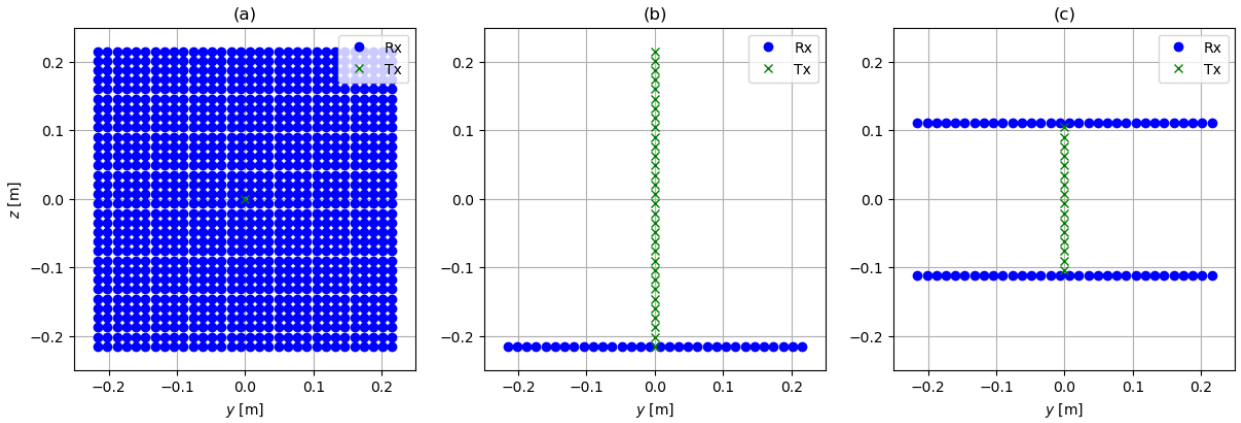

Figure 2: Array arrangements for three different scenarios. (a) SIMO, (b) T-Array, (c) H-Array

to virtual array elements compared to the previously proposed T array. For a complete cost analysis, the cost of one receiver channel and one transmitter channel would need to be known, which is not intended to be in the scope of this work.

For the simulation, a point target is placed in front of each array, allowing the point spread function (PSF) of the array to be determined. The PSF is shown throughout this paper in three projection planes: the azimuth-range plane, the range-elevation plane, and the azimuth-elevation plane, with a common intersection at the position of the target. To evaluate the simulation results, the PSF is divided into the areas of signal backscatter and clutter, from which the signal-to-clutter ratio (SCR) can be determined. In addition, the 3 dB beamwidth of the main lobe in the horizontal and vertical directions is determined, which gives an estimate of the resolution of the system.

Figures 3 to 5 show the simulation results for the three array configurations respectively. As expected, the SIMO case presented in Figure 3 shows a match of the PSF in the range-azimuth plane as well as the range-elevation plane, since the array is square and has the same characteristics in the y- and z-directions. The 3 dB beamwidth is 3.2° in the horizontal and vertical directions, which corresponds to the theoretical beamwidth of

$$\Delta\phi_{3\text{dB}} = 0.88 \cdot \frac{\lambda}{L} \cdot \frac{180^\circ}{\pi} = 0.88 \cdot \frac{0.029\,\text{m}}{0.45\,\text{m}} \cdot \frac{180^\circ}{\pi} = 3.2^\circ, \tag{9}$$

where λ is the wave length and L the aperture length of the array. Regarding the influence of cross-correlation noise on the SCR, this scenario represents the ideal case, since there is no influence of cross-correlation noise by using only one transmitter pulse.

Figure 4 shows the result for the T array. It can be seen that the virtual array also achieves a beam width of 3.2° in horizontal and vertical direction. However, the influence of the cross-correlation noise is now apparent, especially in the vertical plane (cf. Figure 4.b). Here the whole background is filled with clutter, which is caused by the limited pulse separation. This is reflected in a reduction of the SCR by 12.7 dB compared with the SIMO case. The PSF in the range-azimuth plane is barely affected by the cross-correlation noise. Only in the direction of the target the clutter is significantly increased. This can be explained by the given aperture of the receiver module focusing the backscattered energy, i.e. also that of the cross-correlation noise, in the beam in which the target is located.

Figure 5 shows the third scenario, where the H array is used. This setup allows the number of transmitters to be halved and still produce a virtual 32×32 array with a 3 dB horizontal and vertical beamwidth of 3.2°. By halving the number of transmitter pulses, the influence of cross-correlation noise can be reduced by approximately 3 dB as expected. This is particularly reflected in the clutter of the range elevation plane (cf. Figure 5.b). Due to the H array configuration with its two rows of receiver elements, we also can observe an

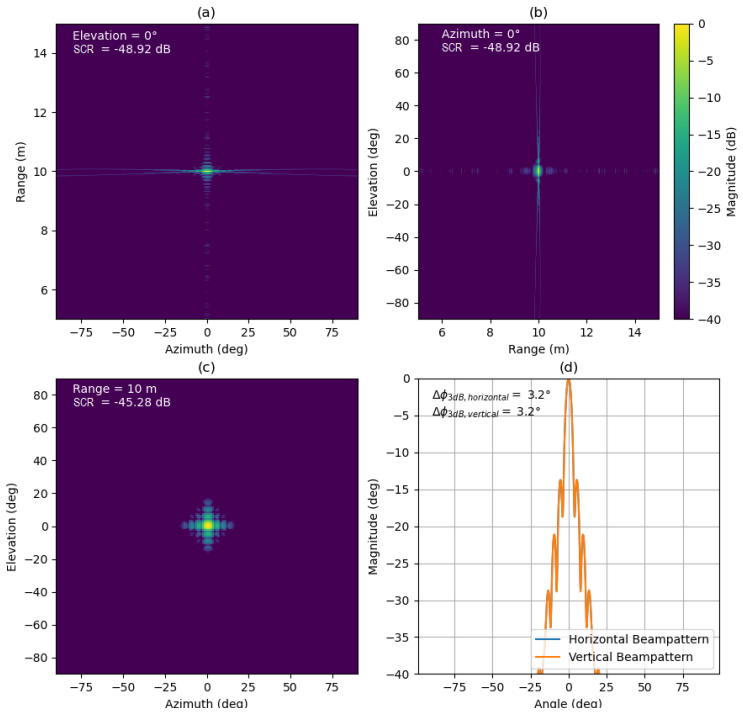

Figure 3: Simulation results for the SIMO-Array-Configuration with the same colorbar in subfigures (a)-(c). (a) Range-azimuth domain, (b) range-elevation domain, (c) azimuth-elevation domain, (d) horizontal and vertical beampattern (horizontal beampattern is hidden by vertical beampattern).

energy focusing of the cross-correlation noise in Figure 5.b as an elevation beampattern, where the zeros of the beampattern appear as dark horizontal lines.

5. EXPERIMENT

A MIMO sonar demonstrator manufactured by ATLAS ELEKTRONIK GmbH was built, which allows an experimental validation of simulations presented above. Due to limitations in the production and costs, the demonstrator does not match the number of channels as used in the simulations, where an ideal quadratic 2D planar array is tested. Instead it consists of a receiver module and four transmitter modules, each with three channels, i.e. $M = 12$ (cf. Figure 6.a). They have a bandwidth of $B = 20$ kHz at a center frequency of $f_c = 50$ kHz. The receiver module is a uniform linear array with $N = 32$ elements, which have a spacing of $d_r = \lambda_c/2$ with $\lambda_c = c/f_c$. They have a bandwidth of 20 kHz at a center frequency of 50 kHz. The four transmitter modules are mounted in a column above the receiver module, forming a T-Array as shown in Figure 6.b. Due to the design of the sonar demonstrator, the transmitter array is not completely allocated, i.e. a spacing of $d_t = \lambda_c/2$ is not maintained, which is why grating lobes are to be expected in the vertical beampattern. Figure 6.c shows the analytical narrow band beampatterns in vertical and horizontal direction.

The experiment takes place in a harbor basin. The water depth is ~6 m and the sonar system is mounted at a depth of 2 m. The speed of sound is estimated to be 1480 m/s. An artificial target is placed approximately 10 m in front of the sonar to determine the PSF of the system. In the experiment, the transmitter pulses shown in Section 3 are emitted via the transmitter array. In the signal processing the receiver signals are mixed in the baseband and seperated by a matched filter bank to enable a link between every transmitter module and receiver channel. These $M \cdot N$ signals are processed in a coherent time domain back projection beamformer, to deduce the direction and range information of the targets.

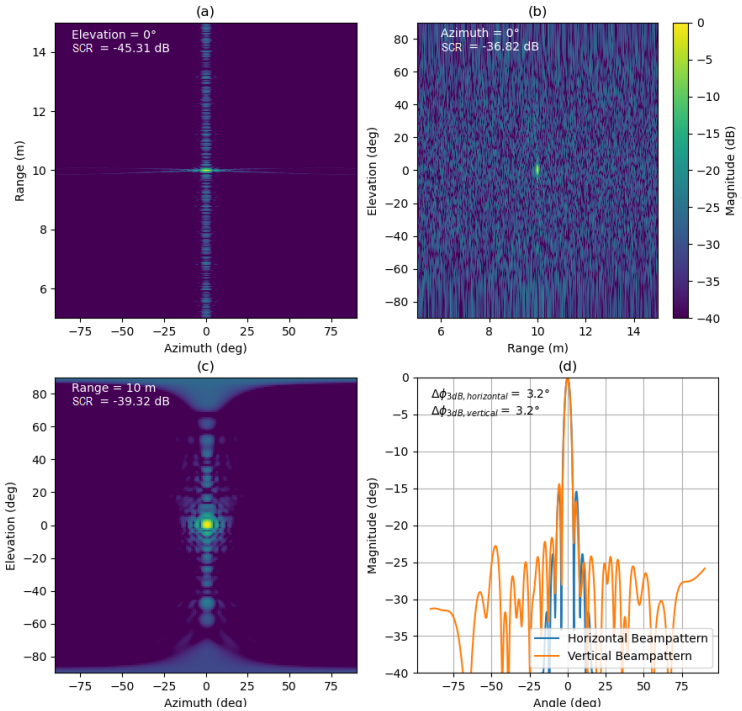

Figure 4: Simulation results for the T-Array-Configuration with the same colorbar in subfigures (a)-(c). (a) Range-azimuth domain, (b) range-elevation domain, showing background clutter caused by cross-correlation noise (c) azimuth-elevation domain, (d) horizontal and vertical beampattern.

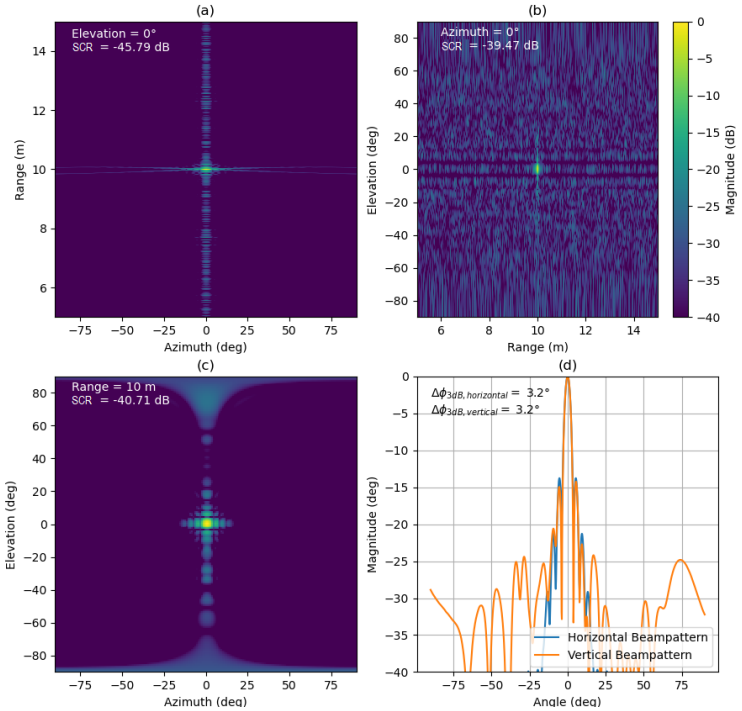

Figure 5: Simulation results for the H-Array-Configuration with the same colorbar in subfigures (a)-(c). (a) Range-azimuth domain, (b) range-elevation domain, (c) azimuth-elevation domain, (d) horizontal and vertical beampattern.

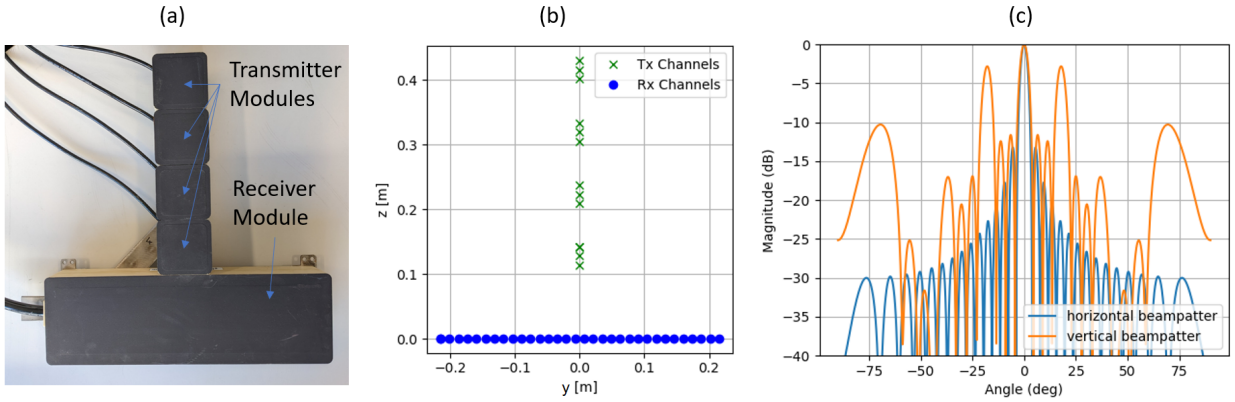

Figure 6: (a) MIMO sonar demonstrator, (b) array arrangement, (c) theoretical vertical and horizontal beampattern

Figure 7 shows the result of the experiment. The test target is located 9.6 m from the sonar, with an azimuth angle of -2° and an elevation angle of -4°. This setup was additionally simulated to serve as a reference under ideal channel conditions (cf. Figure 8). As in the simulations in the previous section, the PSF is shown in three planes, which have a common intersection at the location of the target. Due to the grating lobes in the vertical beampattern of the array, we can observe the target at three different elevation angles, where the upper and lower targets are ghost targets. Thereby the ghost targets appear at different ranges (cf. Figure 7.b), which can be explained by the asymmetrical setup in the experiment. For this reason, the ghost targets are not appearing in Figure 8.c and Figure 8.d or just partially in Figure 7.c and Figure 7.d, because these subfigures showing the results for the specific range of 9.6 m.

In contrast to the simulation, where an ideal acoustic channel was considered, the experiment is in a non-ideal environment where reverberation at the water surface, the seafloor and the water volume significantly affect the SCR in the measurement. Thus, the acoustic reverberation in each plane (Figure 7.a - 7.c) causes clutter in the background. Comparing the results from Figure 7 with the reference from the simulation, it can be seen that especially the SCR in the range-azimuth plane is significantly degraded. However, the properties of the array like the location of ghost targets in the subfigures (b) (caused by grating lobes in the vertical beampattern) and the beamwidth of the main lobe in the subfigures (d) show a high level of agreement when comparing the theoretical model (cf. Figure 6.c) and the simulated reference (cf. Figure 8.d). Thus, the experiment validates the functionality of the proposed vertical stacked virtual array.

6. SUMMARY

In this paper, the MIMO sonar principle as well as the concept of a virtual array for the realization of a virtual planar sonar array were investigated in detail. For this purpose, a simulation of the acoustic MIMO channel was developed, which allowed an observation of different array configurations under ideal conditions. Thereby the simulations are focused on a standard 32×32 planar array, which is a likely configuration for future applications. In addition, a MIMO sonar test array was built and used for experiments in a realistic environment. For the operation of a MIMO sonar, pulse separation becomes a key issue. Therefore, a set of OFDM pulses were designed in this work, which allows the simultaneous operation of multiple transmitters. To analyze the virtual array, the 3 dB width of the response of a single point scatterer and the level of background clutter is evaluated and compared to a simulated SIMO reference. Simulations and experiment show that the virtual planar array can achieve the expected 3dB beamwidth both vertically and horizontally. However, the OFDM pulse form design directly translates into background clutter due to cross-correlation noise, so pulse separation remains an important variable for future work in this area.

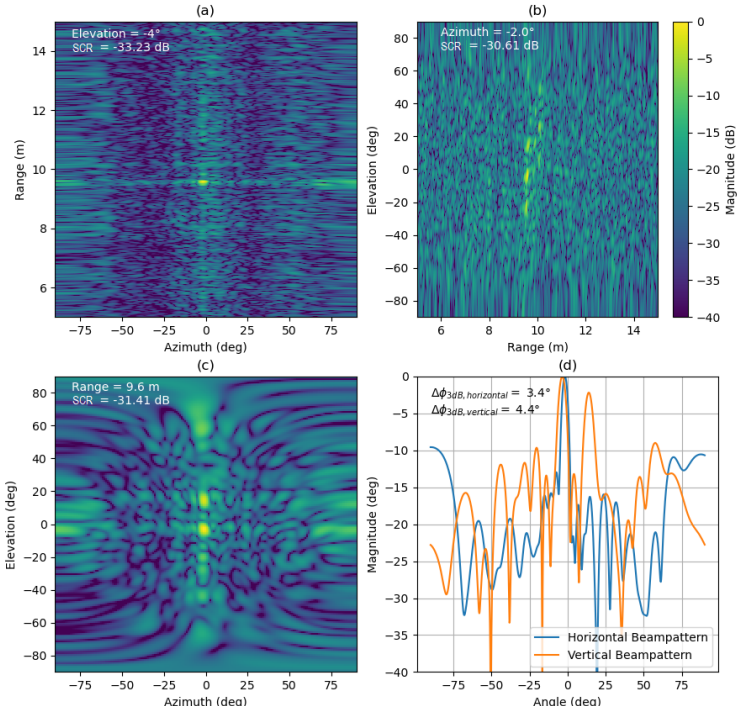

Figure 7: Experiment results. (a) Range-azimuth domain, (b) range-elevation domain, (c) azimuth-elevation domain, (d) horizontal and vertical beampattern.

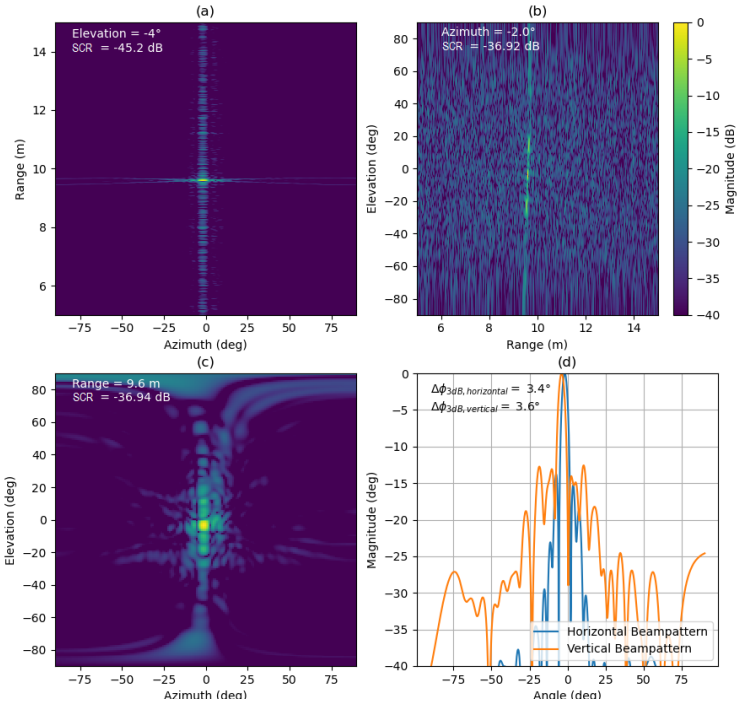

Figure 8: Results of simulated setup. (a) Range-azimuth domain, (b) range-elevation domain, (c) azimuth-elevation domain, (d) horizontal and vertical beampattern.

REFERENCES

[1] R.C. Trider, "Signal Investigation for Low Frequency Active (LFA) Sonar", *Defence Research and Development Canada*, (2012).

[2] J. Li & P. Stoica, "MIMO Radar Signal Processing", *John Wiley & Sons*, (2009).

[3] Y. Pailhas, Y. Petillot, K. Brown & B. Mulgrew, "Spatially Distributed MIMO Sonar Systems: Principles and Capabilities", *IEEE Journal of Oceanic Engineering* **42**, 738-751 (2017).

[4] J. Li & P. Stoica, "MIMO Radar with Colocated Antennas", *IEEE Signal Processing Magazine*, **24**, 106-114 (2007).

[5] S. Schröder, Z. Qiao, D. Kraus & N. Theuerkauf, "Investigation of the resolution enhancement achieved by MIMO Sonar systems", *Jahrestagung für Akustik DAGA*, (2018).

[6] S. Schröder, J. Reermann, M. Stephan, D. Kraus, & A. Kummert. " Experimental demonstration of the angular resolution enhancement of a monostatic MIMO sonar". *In Proceedings of Meetings on Acoustics UACE (Vol. 44, No. 1, p. 070009). Acoustical Society of America*, (2021).

[7] Y. Pailhas, Y. Petillot, "Wideband CDMA Waveforms for Large MIMO Sonar Systems", *2015 Sensor Signal Processing for Defence (SSPD)*, 1-4 (2015).

[8] Z. Qiao, M. Buß, C. Zimmer, D. Kraus & A. M. Zoubir, "Investigation on Point Spread Function of MIMO SAS with Frequency Modulated Waveforms", *OCEANS 2018 MTS/IEEE Charleston*, 1-8 (2018).

[9] G. Hakobyan, "Orthogonal frequency division multiplexing multiple-input multiple-output automotive radar with novel signal processing algorithms.", *PhD Thesis*, University of Stuttgart, Germany, (2018).